Journal of Engineering Science and Technology
Vol. 21, No. 3 (2026) 871 - 879

INFLUENCE OF CUTTING SPEED, POWER, AND GAS PRESSURE ON HEAT AFFECTED ZONE FORMATION AND MICROSTRUCTURAL EVOLUTION IN LASER-CUT MILD STEEL

H. HANIZAM[1,*], M.A. CHE AHMAD[2], N. MOHAMAD[1], N. BAHIYAH BABA[3]

[1]Fakulti Teknologi dan Kejuruteraan Industri dan Pembuatan, Universiti Teknikal Malaysia Melaka, Hang Tuah Jaya, Durian Tunggal Melaka 76100, Malaysia
[2]Operation and Production Department, Volcan Engineering Solution Sdn. Bhd., Setia Mayuri, 43500 Semenyih, Selangor, Malaysia
[3]Faculty of Engineering Technology, University College TATI (UC TATI), Teluk Kalong, Kemaman 24000, Terengganu, Malaysia
*Corresponding Author: hanizam@utem.edu.my

Abstract

Laser cutting induces a Heat Affected Zone (HAZ) in mild steel, characterized by microstructural alterations that compromise mechanical properties. This study investigates the effect of laser power parameters on the HAZ characteristics of thick ASTM A36 mild steel. Hardness was measured at incremental distances from the cut edge (2–25 mm), and microstructural analysis was conducted using optical microscopy. Results demonstrated that all parameter settings produced a consistent HAZ extending approximately 4–6 mm from the cut. A significant hardness reduction of up to 9.4% was observed at 2 mm, attributed to grain coarsening and dominant ferrite formation due to slow cooling. Hardness recovered to base material levels (77.5 HRB) by 25 mm. Statistical analysis (t-test, α=0.05) confirmed that studied laser parameter settings did not significantly influence the final HAZ size or hardness distribution, indicating that HAZ formation is an inherent result of the thermal process rather than parameter variation. These findings provide critical insight for industry, confirming that component design must account for this predictable softened region.

Keywords: Heat affected zone, Laser cutting, Mild steel, T-Test.

1. Introduction

Laser cutting, a cornerstone of modern precision manufacturing, utilizes high-power-density beams to melt, vaporize, or ablate materials with exceptional accuracy [1, 2]. However, this process inherently introduces localized thermal cycles, resulting in rapid expansion and contraction that can disturb the material's microstructural integrity adjacent to the cut edge. This thermally altered region, known as the Heat Affected Zone (HAZ), is characterized by gradients in microstructure, residual stress, and mechanical properties such as hardness, which often differ significantly from the base material [3, 4]. These unpredictable property gradients can compromise the in-service performance and structural reliability of components, making the HAZ a critical consideration for safety-critical applications.

The optimization of the HAZ is particularly relevant for mild steel, a material prized in construction, automotive, and heavy industries for its cost-effectiveness, weldability, and balanced mechanical properties [5, 6]. Its expanding application into high-stress components such as gears, turbine blades, and seismic-resistant structures necessitates stringent quality control [7, 8].

In laser cutting, the geometry and severity of the HAZ are predominantly governed by a triad of process parameters: laser power, cutting speed, and assist gas pressure [9, 10]. Mamman et al. [11] stated that these factors exhibit complex interdependencies; for instance, while higher cutting speeds can reduce HAZ width, they may simultaneously impair cut quality by promoting striations or dross adhesion.

Conversely, Ceritbinmez et al. [12] concluded that excessive laser power intensifies thermal input, exacerbating microstructural degradation such as grain coarsening. Zhou et al. [13] reported that the micro hardness near laser-textured areas on YG6 cemented carbide decreases due to the laser-induced coarsening of tungsten carbide (WC) grains. In addition, Basak et al. [14] found that HAZ width depends non-linearly on laser power, cutting speed, and focus position, but linearly on assist gas pressure. The selection of optimal parameters is therefore essential to balance productivity with final component performance.

Previous research underscores the significance of these parameters. Studies on materials like 22MnB5 boron steel have demonstrated that CO_2 laser power alone can cause HAZ thickness variations from 116.03 μm to 326.42 μm by Tahir and Rahim [15]. Furthermore, cutting speed demonstrates an inverse relationship with HAZ size, while assist gas pressure is critical for efficient melt ejection and directly influences cut quality and thermal diffusion [16-18]. For 6 mm mild steel, this requires precise calibration of standard CO_2 systems (typically $\leq$4000 W) to achieve a clean cut with a minimized HAZ according to Jain et al. [19].

Quantifying the effect of parameter settings requires robust statistical methods. The t-test is particularly advantageous for industrial research with limited sample sizes, offering a rigorous framework for detecting statistically significant differences in mean material properties, such as hardness, across different processing conditions.

This study investigates the influence of low, medium, and high laser cutting parameter regimes on the hardness distribution and microstructural evolution within the heat-affected zone (HAZ) of 6 mm ASTM A36 mild steel plate. Selected for its widespread structural use due to favourable cost and mechanical properties,

A36 typically exhibits a ferrite-pearlite microstructure, with its exact phase balance and grain size determined by processing history and cooling conditions.

Hardness mappings were conducted at incremental distances from the cut edge to quantitatively delineate the HAZ extent. Variations in hardness and microstructure across parameter sets were rigorously evaluated for statistical significance using t-tests. The findings provide practical, data-driven insights for industrial laser-cutting optimization, with the aim of minimizing HAZ alteration and enhancing cut-component reliability.

2. Experimental Procedures

2.1. Material and equipment

Experiments were conducted on 6 mm-thick ASTM A36 low-carbon structural steel, a material chosen for its widespread industrial use and cost-effectiveness. A CO_2 laser cutting system (Model FO MII 3015 NT, Amada America, Inc.) employing nitrogen (N_2) assist gas was used for the cutting process as shown in Fig. 1. The machine was configured with the following standard parameters: a frequency of 2000 Hz, a nozzle diameter of 1.2 mm, a nozzle gap of 0.7 mm, and a focus point of -2.5 mm. All samples were cut into uniform 50 mm × 50 mm squares.

Fig. 1. CO_2 Laser machine.

2.2. Cutting strategy

Table 1 details the three laser parameter settings investigated, with five samples manufactured per setting. Hardness measurements were taken at specified distances (2, 4, 6, 8, 10, 15, 25 mm) from the cut edge, denoted as Distance Away from Cut (DAC). Twenty measurements were obtained for each parameter setting. The statistical significance of differences between parameter settings was assessed using a two-sample t-test in Minitab (significance level: $\alpha = 0.05$).

Table 1. Laser cutting parameter setups.

Parameter	Low	Medium	High
Cutting Speed, mm/s	800	1200	1500
Laser Power, W	1900	2300	2700
Gas Pressure, MPa	0.08	0.09	0.1

2.3. Characterizations

The samples were prepared for analysis using standard metallographic procedures. All surfaces were ground and polished using standard kits, then etched with a 2% Nital solution (a mixture of nitric acid and ethanol) for 5 seconds to reveal the microstructure. Microstructural analysis was conducted using a Leica DVM6 digital microscope.

Prior to mechanical testing, the samples were cleaned and lightly reground with 800-grit sandpaper to ensure a smooth, rust-free surface for accurate hardness measurements. Hardness testing was subsequently performed using a Mitutoyo Rockwell hardness tester (Model HR-430MR) with a 1/16" steel ball indenter and an HRB scale under a major load of 100 kg. Figure 2 shows a representative sample after hardness testing.

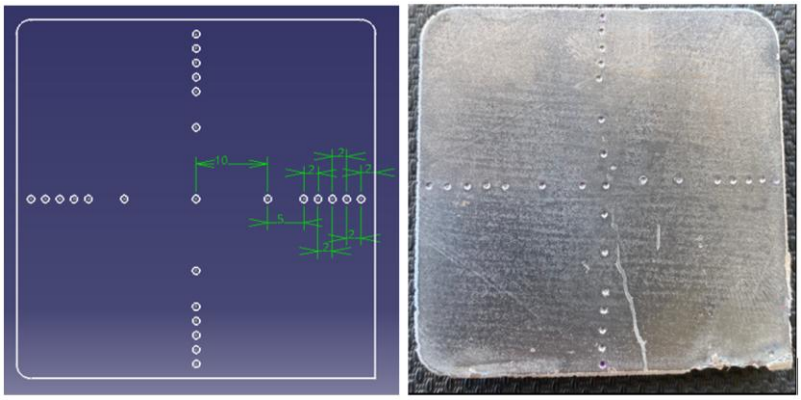

Fig. 2. Example of sample hardness test of (a) plan and (b) actual.

3. Results and Discussion

3.1. Heat affected zone analysis based on hardness

The hardness of the HAZ in laser-cut mild steel was evaluated under low, mid, and high parameter settings. Hardness samples were examined at distances of 2, 4, 6, 8, 10, 15, and 25 mm away from the cut edge (DAC), as presented in Fig. 3. All parameter settings (low, mid, and high) exhibited nearly identical hardness trends across all measured points, plateauing by 15 mm DAC. The lowest hardness values were recorded at 2 mm DAC, measuring 71.3 HRB, 70.28 HRB, and 70.20 HRB for the low, mid, and high settings, respectively. These values then increased significantly to a range of 75.38 - 75.83 HRB at 4 mm DAC. Subsequently, the hardness gradually increased further, reaching 76.29 – 77.38 HRB at 15 mm DAC.

By 25 mm DAC, the hardness values approached that of the uncut base mild steel (77.5 HRB), indicating the end of the HAZ. The maximum hardness reduction at 2 mm DAC, compared to the base material, was 8.0%, 9.3%, and 9.4% for the low, mid, and high settings, respectively. This observed softening is consistent with trends reported in literature; for instance, Basak et al. documented hardness reductions of 22.7% and 20.5% in the HAZ of mild steel and stainless steel cut with a fibre laser, respectively. Zhou et al. also found that the microhardness of the cemented carbide at a 10 μm depth was reduced by 17.9% from its base value.

This phenomenon is attributed to microstructural alterations caused by localized heat and thermal cycles. The heat from cutting leads to grain coarsening and a reduction in dislocation density, which softens the material. Furthermore, the slow cooling conditions promote the formation of soft ferrite over the harder pearlite, which dissolved during the initial heating phase. Therefore, the formation of a HAZ in mild steel is significant, extending approximately 4 mm from either side of the cutting edge, as this is the region where the most substantial microstructural changes and hardness reduction occur.

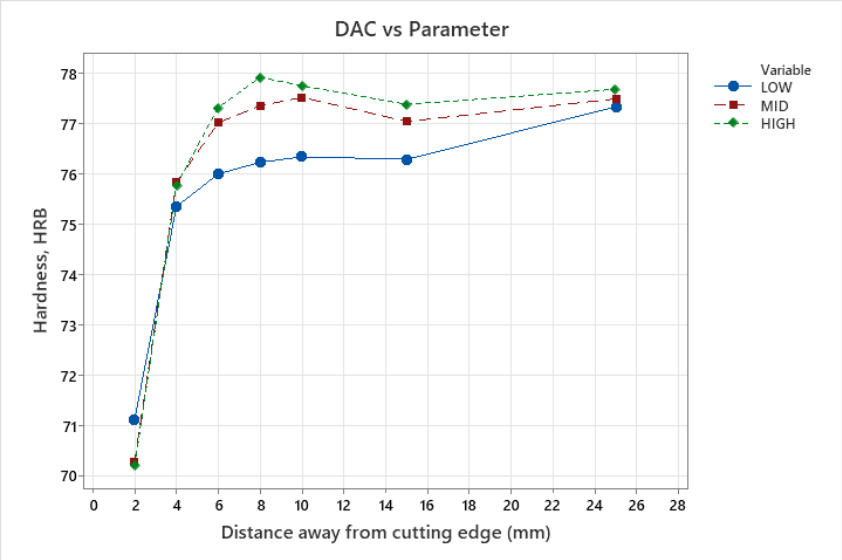

Fig. 3. Average hardness versus distance from the cutting edge.

3.2. Heat affected zone microstructures

Figure 4 depicts the heat-affected zone (HAZ) of mild steel following laser cutting. This region exhibits distinct microstructural changes due to variations in cooling rate. Near the cutting edge (within 1–2 mm), the material experiences the most intense heat input and the slowest cooling rate. This thermal cycle promotes the extensive formation of ferrite (α-Fe), with only minor precipitation of cementite (Fe_3C). As shown in Figs. 4(a) and (b), these ferrite-dominated regions appear dark under optical microscopy because the lack of fine pearlite lamellae that reduces light scattering. Ferrite is a soft and ductile body-centred cubic (BCC) phase; its dominance in this zone results in lower hardness and wear resistance.

At approximately 4 mm from the cut, the material experiences a lower peak temperature and a comparatively faster cooling rate. This optimal thermal cycle facilitates the near-complete transition of the microstructure to pearlite, as seen in Figs. 4(c) and (d). Pearlite forms via the decomposition of austenite into alternating thin lamellae of ferrite and cementite. Since pearlite is harder than ferrite, the mechanical properties, particularly hardness and strength increase progressively with distance from the cut edge. Beyond this region, the peak temperature falls below the transformation range, leaving the original, unaffected base metal microstructure, which typically consists of ferrite and pearlite.

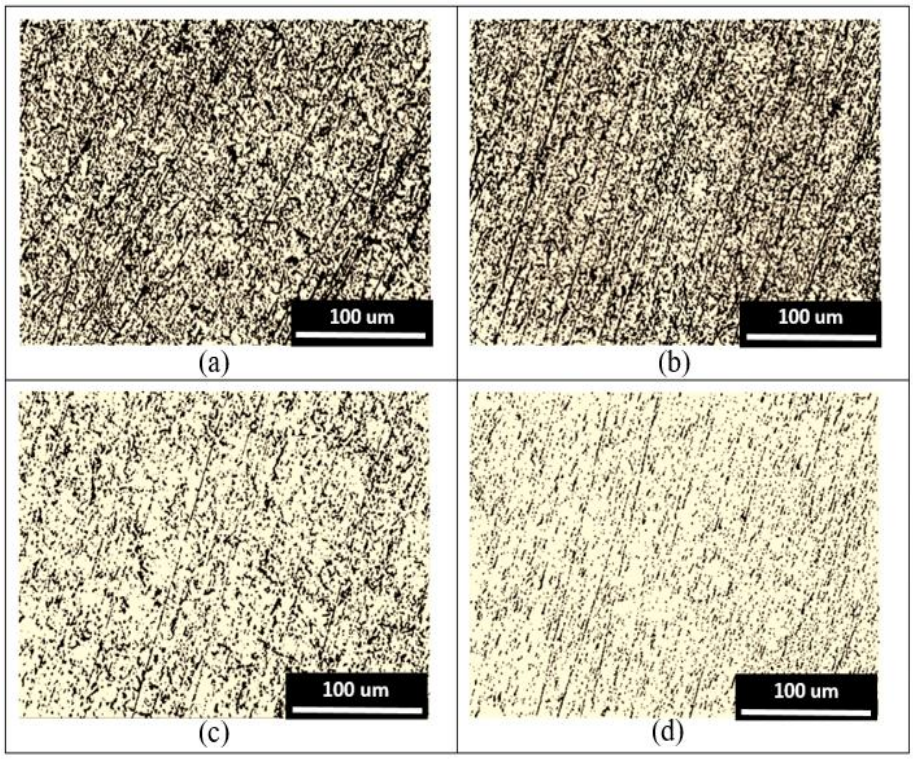

Fig. 4. Heat affected zone microstructure of low carbon steel at slow cooling at (a) 1 mm, (b) 2mm, (c) 4 mm and (d) 6 mm, distance away from cutting edge.

3.3. T-test analysis

Significant hardness gradients were observed from 2 mm to 4 mm from the cut edge (DAC), with values of 75.35 HRB, 75.83 HRB, and 75.78 HRB for the low, mid, and high parameter settings, respectively (Fig. 2). A substantial increase in hardness was then recorded at 6 mm DAC, with values of 76.00 HRB, 77.02 HRB, and 77.32 HRB for the same settings. Beyond this point, the hardness values plateaued up to 25 mm DAC.

To identify the parameters with a significant influence, a two-sample t-test for means was conducted. Table 2 presents the t-test results comparing the low vs. mid, mid vs. high, and low vs. high parameters at 4 mm and 6 mm DAC. The p-values for nearly all comparisons exceeded 0.05, indicating no statistical significance. The only exception was the comparison between the low and high parameters at 6 mm DAC, which yielded a p-value of 0.027.

Therefore, this analysis suggests that the laser parameter settings do not play a significant role in extending the heat-affected zone (HAZ) in mild steel. The HAZ consistently extends up to 6 mm from the cutting edge, provided the laser cutting operation is successful.

Table 2. P-values at 4 mm and 6 mm DAC.

Sample	N	Mean	StDev	SE Mean	P-Value
LOW-DAC4	12	75.35	1.2	0.35	
					0.413
MID-DAC4	12	75.83	1.56	0.45	
					0.951
HIGH-DAC4	12	75.78	1.71	0.49	
					0.481
LOW-DAC4	12	75.35	1.2	0.35	
LOW-DAC6	12	76	1.33	0.38	
					0.061
MID-DAC6	12	77.02	1.18	0.34	
					0.574
HIGH-DAC6	12	77.32	1.38	0.4	
					0.027
LOW-DAC6	12	76	1.33	0.38	

Remark: DAC4/6 – refer to 4 mm and 6 mm distance away from cutting edge.

4. Conclusions

The findings of this study demonstrate that laser cutting induces a consistent heat-affected zone (HAZ) in mild steel, characterized by distinct hardness variations across different distances from the cut edge (DAC). All parameter settings (low, medium, and high) exhibited similar hardness trends, with the lowest values occurring closest to the cut (2 mm DAC) due to thermal softening effects. The hardness showed a sharp recovery at 4 mm DAC (75.38-75.83 HRB) and gradually increased to near-base material levels (77.5 HRB) by 25 mm DAC.

Microstructural analysis revealed that this softening near the cut edge results from slow cooling conditions that promote ferrite formation, while the hardness recovery correlates with increased pearlite content farther from the cut. Although higher parameter settings showed slightly greater hardness reductions (9.4% for high vs. 8.0% for low parameters), statistical analysis confirmed no significant differences in hardness between parameter groups at 2 mm DAC ($p > 0.05$ for all comparisons). These results indicate that the initial HAZ softening is primarily governed by thermal effects rather than laser power variations.

The study establishes that the most significant microstructural changes occur within 4 mm of the cut edge, providing valuable insights for industrial applications where HAZ control is critical. Future research could investigate methods to minimize HAZ softening through controlled cooling techniques or explore the effects of different steel compositions on HAZ characteristics. This work contributes to a better understanding of HAZ formation in laser-cut mild steel and provides a foundation for optimizing cutting parameters in precision manufacturing applications.

Acknowledgments

The authors would like to extend a special thank you to the Centre for Research and Innovation Management (CRIM), Fakulti Teknologi dan Kejuruteraan Industri

dan Pembuatan, Universiti Teknikal Malaysia Melaka, and Malaysian Ministry of Higher Education

References

1. Sang, S.; Zhou, K.; Zhou, Y.; Wang, C.; Dai, Y.; and Yu, Z. (2023). Principle, present situation, and development trend of laser cutting. *International Conference on Optoelectronic Materials and Devices* (*ICOMD* 2022), 12600, 12600B, 1-5.
2. Moradi, M.; Moghadam, M.K.; Shamsborhan, M.; Bodaghi, M.; and Falavandi, H. (2020). Post-processing of FDM 3D-printed polylactic acid parts by laser beam cutting. *Polymers*, 12(3), 550.
3. Nguyen, T.H.; Lin, C.K.; Tung, P.C.; Nguyen-Van, C.; and Ho, J.R. (2020). An extreme learning machine for predicting kerf waviness and heat affected zone in pulsed laser cutting of thin non-oriented silicon steel. *Optics and Lasers in Engineering*, 134, 106244.
4. Coronado-Alba, C.E.; Mejía, I.; and Cabrera, J.M. (2021). Metallographic, structural, and mechanical characterization of weld nuggets in Fe–Mn–Al–C low-density steels microalloyed with Ti/B and Ce/La by gas tungsten arc welding process. *Steel Research International*, 92(11), 2100229.
5. Ibeji, C.U.; Akintayo, D.C.; Oluwasola, H.O.; Akintemi, E.O.; Onwukwe, O.G.; and Eziomume, O.M. (2023). Synthesis, experimental and computational studies on the anti-corrosion performance of substituted Schiff bases of 2-methoxybenzaldehyde for mild steel in HCl medium. *Scientific Reports*, 13(1), 3265.
6. Aziz, A.A.; Khalid, E.A.; Alwan, A.S.; and Jaddoa, A.A. (2020). The effect of Nd-YAG laser surface treatment on mechanical properties of carburizing steel AISI 1006. *Journal of Engineering Science and Technology*, 15(6), 3891-3902.
7. Hossain, N.; Chowdhury, M.A.; Masum, A.A.; Islam, M.S.; Shahin, M.; Irfan, O.M.; and Djavanroodi, F. (2021). Effects of self-lubricant coating and motion on reduction of friction and wear of mild steel and data analysis from machine learning approach. *Materials*, 14(19), 5732.
8. Tian, Z.; Sun, J.; Zhao, Y.; Luo, Y.; Liang, Y.; Li, W.; Zhai, M.; Li, J.; Li, Y.; and He, J. (2019). Test comparison and performance analysis of two kinds of almonds shell kernel sorting equipment. *IOP Conference Series*: *Earth and Environmental Science*, 358(5), 052044.
9. Hu, J.; and Zhu, D. (2018). Experimental study on the picosecond pulsed laser cutting carbon fiber reinforced plastics. *Journal of Reinforced Plastics and Composites*, 37(15), 993–1003.
10. Masoud, F.; Sapuan, S.M.; Ariffin, M.K.A.M.; Nukman, Y.; and Bayraktar, E. (2021). Experimental analysis of heat-affected zone (HAZ) in laser cutting of sugar palm fiber reinforced unsaturated polyester composites. *Polymers*, 13(5), 706.
11. Mamman, C.; Isaac, O.E.; and Nkoi, B. (2022). Investigating the effect of cutting speed on heat affected zone in laser cutting process of stainless steel. *International Journal of Engineering and Modern Technology*, 8(4), 25–32.
12. Ceritbinmez, F.; and Yapici, A. (2022). An investigation on cutting of the MWCNTs doped composite plates by CO_2 laser beam. *Aircraft Engineering and Aerospace Technology*, 94(2), 279–288.

13. Zhou, L.; Zou, P.; Yang, Z.; and Ren, B. (2025). Influence of laser texturing parameters on the surface characteristics and cutting performance of cemented carbide tools. *Optics and Laser Technology*, 188, 112933.
14. Basak, A.K.; Lightbody, K.; and Pramanik, A. (2025). The effect of material intrinsic properties on the quality of machined surface during laser beam cutting. *Materials Chemisrty and Physics*, 336, 130546.
15. Tahir, A.F.M.; and Rahim, E.A. (2016). A study on the laser cutting quality of ultra-high strength steel. *Journal of Mechanical Engineering and Sciences*, 10(2), 2145-2158.
16. Kukiełka, L.; Patyk, R.; Bohdal, L.; Napadłek, W.; Gryglicki, R.; and Kasprzak, P. (2019). Investigations of polypropylene foil cutting process using fiber Nb: YAG and diode Nd:YVO4 lasers. *Acta Mechanica et Automatica*, 13(2), 107–112.
17. Kim, K.; Kang, N.; Kang, M.; and Kim, C. (2021). Assessment of heat-affected zone softening of hot-press-formed steel over 2.0 GPa tensile strength with bead-on-plate laser welding. *Applied Sciences*, 11(13), 5774.
18. Orazi, L.; Darwish, M.; and Reggiani, B. (2019). Investigation on the inert gas-assisted laser cutting performances and quality using supersonic nozzles. *Metals*, 9(12), 1257.
19. Jain, P.S.; Varsi, A.M.; Patel, D.S.; and Kagzi, S.A. (2023). Theoretical and experimental investigations for geometrical error during hemispherical cavity machining of CO_2 laser. *Proceedings of the Institution of Mechanical Engineers*, *Part B*: *Journal of Engineering Manufacture*, 237(8), 1139–1148.